NeuroImage **15,** 719–726 (2002)
doi:10.1006/nimg.2001.1005, available online at http://www.idealibrary.com on IDEAL®

RAPID COMMUNICATION

An Investigation of the Value of Spin-Echo-Based fMRI Using a Stroop Color–Word Matching Task and EPI at 3 T

David G. Norris,[1] Stefan Zysset, Toralf Mildner, and Christopher J. Wiggins

Max-Planck-Institute for Cognitive Neuroscience, Stephanstrasse 1a, D-04103 Leipzig, Germany

Received June 8, 2001

This study examines the value of spin-echo-based fMRI for cognitive studies at the main magnetic field strength of 3 T using a spin-echo EPI (SE-EPI) sequence and a Stroop color–word matching task. SE-EPI has the potential advantage over conventional gradient-echo EPI (GE-EPI) that signal losses caused by dephasing through the slice are not present, and hence although image distortion will be the same as for an equivalent GE-EPI sequence, signal voids will be eliminated. The functional contrast in SE-EPI will be lower than for GE-EPI, as static dephasing effects do not contribute. As an auxiliary experiment interleaved diffusion-weighted and non-diffusion-weighted SE-EPI was performed in the visual cortex to further elucidate the mechanims of functional contrast. In the Stroop experiment activation was detected in all areas previously found using GE-EPI. Additional frontopolar and ventral frontomedian activations were also found, which could not be detected using GE-EPI. The experiments from visual cortex indicated that at 3 T the BOLD signal change has contributions from the extravascular space and larger blood vessels in roughly equal amounts. In comparison with GE-EPI the absence of static dephasing effects would seem to result in a superior intrinsic spatial resolution. In conclusion the sensitivity of SE-EPI at 3 T is sufficient to make it the method of choice for fMR studies that require a high degree of spatial localization or where the requirement is to detect activation in regions affected by strong susceptibility gradients.

INTRODUCTION

The use of T_2 contrast in functional magnetic resonance imaging (fMRI) offers two possible advantages in comparison with the more commonly used T_2^* contrast: First, T_2 varies far less through the brain than does T_2^* and hence the degree of functional activation may be more readily compared between brain regions. Second, T_2-weighted imaging sequences do not suffer from signal voids caused by imperfect slice rephasing due to through-plane susceptibility gradients. In-plane susceptibility gradients which are strong enough to remove the signal from the acquisition window in a gradient-echo sequence will be refocused and hence give no signal loss. However, if the EPI imaging sequence is employed the depiction of such regions may suffer considerable distortion. It is also possible to use imaging sequences such as those based on RARE (Hennig *et al.*, 1986) which do not suffer from image distortion (Constable *et al.*, 1994). The quality of functional contrast obtained with T_2-weighted imaging differs from that of T_2^*-weighted images in that all contributions from static dephasing are eliminated. This considerably reduces the magnitude of the signal change that can be obtained, and for this reason T_2-weighted BOLD imaging has to date found limited use, being confined to functional studies of the primary cortices (Bandettini *et al.*, 1994; Constable *et al.*, 1994; Thulborn *et al.*, 1997; Jones *et al.*, 1998; Jones, 1999; Oja *et al.*, 1999; Lee *et al.*, 1999; Lowe *et al.*, 2000) or to signal changes resulting from physiological stress (Prinster *et al.*, 1997; van Zijl *et al.*, 1998; Kavec *et al.*, 2001).

There are three primary mechanisms that can contribute to BOLD signal changes in T_2-weighted imaging:

1. extravascular dynamic averaging,
2. intravascular dynamic averaging, and
3. intravascular changes in T_2.

The first two of these are expected to vary in strength with the square of the static magnetic field strength $\mathbf{B}_0$. It has been convincingly argued by van Zijl *et al.* (1998) that in the intravascular compartment T_2

[1] Present address: F. C. Donders Centre for Cognitive Neuroimaging, Trigon 181, P.O. Box 9101, NL-6500 HB Nijmegen, The Netherlands.

1053-8119/02 $35.00

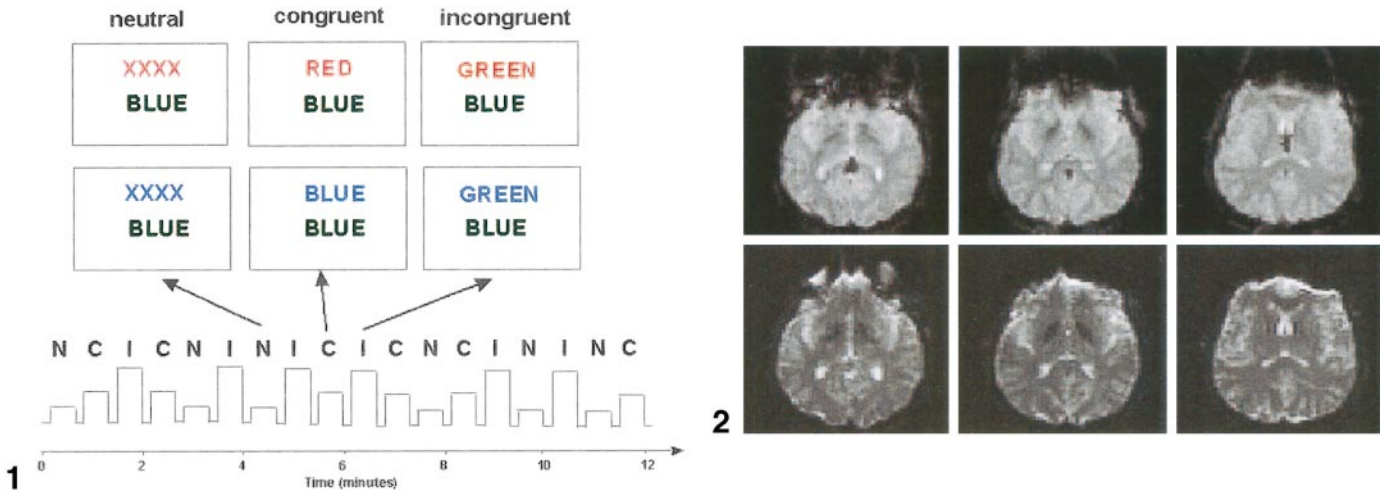

FIG. 1. Stroop experimental design. The three experimental conditions, neutral (N), congruent (C), and incongruent (I), are shown. In each condition volunteers had to determine whether the color of the upper characters corresponded to the meaning of the lower word. In the top three instances the correct answer would be "No," in the bottom three it would be "Yes." The lower part of the diagram shows a pseudo-random presentation scheme and a representation of the corresponding design file.

FIG. 2. GE-EPI (top) and SE-EPI (bottom) images obtained in succession from the same subject showing the reduced signal loss in frontal regions with SE-EPI.

changes dominate. However, the T_2 of venous blood decreases significantly faster than that of gray matter with increasing field strength (Wright *et al.*, 1991), so it is to be expected that the relative importance of the first mechanism will increase substantially with increasing $\mathbf{B}_0$. This has been substantiated in a number of experiments, which have shown that at 1.5 T T_2-weighted BOLD is either exclusively (Oja *et al.*, 1999) or primarily due to intravascular signal changes (Jones, 1999), whereas at 9.4 T the intravascular contribution is negligible (Lee *et al.*, 1999). It is clear that signal both from larger blood vessels and from the paryncheme can be seen in T_2-weighted BOLD imaging (Prinster *et al.*, 1997); however, in a previous study performed at 3 T it was possible to show an improved spatial resolution in the visual cortex compared to T_2^*-weighted imaging (Thulborn *et al.*, 1997). This improvement manifests itself in the ability of spin-echo methods to discriminate positive and negative bands of activation in V1/V2 in response to the vertical motion of a checkered matrix which are not discernable in a gradient-echo sequence having the same resolution. The purpose of this study is to examine whether it is possible to use T_2-weighted BOLD imaging at the main magnetic field strength of 3 T for cognitive studies and not just for examining the primary cortices. To this end, multislice spin-echo EPI (SE-EPI) is used in a Stroop color–word matching task. This Stroop experiment is known to produce robust activation in a number of brain regions (Zysset *et al.*, 2001). The specific aims are then to verify that the same regions are activated as are seen with gradient-echo EPI (GE-EPI) as reported in the previous study (Zysset *et al.*, 2001), to qualitatively compare the activations obtained and to examine whether new regions of activation can be detected in locations which suffer from signal voids in GE-EPI experiments, although the main loci of activation in a Stroop experiment are not necessarily to be expected in these regions. Additionally the results of auxiliary experiments in the visual cortex will be reported, which give some indication as to the origin of BOLD T_2 changes at 3 T. In these experiments event-related activation in the visual cortex is examined using either interleaved diffusion-weighted and non-diffusion-weighted spin-echo EPI or non-diffusion-weighted spin-echo EPI. An event-related design makes it possible to examine both the BOLD signal change and any poststimulus undershoot. It has recently been shown that the balloon model (Buxton *et al.*, 1998) may successfully be applied to model BOLD signal responses at 3 T (Mildner *et al.*, 2001), and hence any poststimulus undershoot may be interpreted as indicating an extravascular contribution. The interleaved diffusion-weighted measurement was performed to examine the relative contributions of the intra- and extravascular compartments without suffering from intertrial variability. In this way it is possible to separate the response from postcapillary vessels, which will be suppressed by the diffusion weighting, from that arising from smaller vessels and the parenchyma, which diffusion weighting will not eliminate.

METHODS

All experiments were performed using a 3-T whole body scanner (Bruker Medical, Ettlingen, Germany). A birdcage resonator of 28 cm i.d. was used for RF trans-

mission and signal reception. The maximal gradient strength was 45 m T/m, switchable within 320 μs.

Stroop Experiment

Subjects

Written consent was obtained from all seven subjects (all right handed, 23–31 years of age, three female) prior to the scanning session. All subjects had normal or corrected-to-normal vision, had normal color vision, and were native German speakers. No subject had a history of neurological, major medical, or psychiatric disorder; none were taking medication at the time of measurement.

Psychophysical Procedures

An adapted single-trial version of the color–word interference task adapted from Treisman and Fearnley (1969) was used. The task was presented using a blocked design and has previously been described in detail (Zysset *et al.*, 2001). Briefly, the experiment can be understood by reference to Fig. 1, which shows the three conditions involved in the task. In each condition the subject had to determine whether the color of the top row matched the color word on the bottom row (printed in black). In the neutral condition the top row just contained a row of four X's, in the congruent condition the top row had a color word printed in the corresponding color, whereas in the incongruent condition the color word was printed in a noncorresponding color. For illustrative purposes English words are used in Fig. 1, whereas in practice German was employed.

For the color–word Stroop task, six neutral blocks alternated with six congruent and six incongruent blocks for each run. Between each condition block, a resting baseline of 10 was introduced. Each stimulus was presented and, if no response was given after a maximal time of 1.5 s, the next trial was presented. If a response was given, the stimulus disappeared and the residual time was filled by a blank screen. Given a fixed interstimulus interval of 1.5 s, subjects completed 20 trials during each (neutral/congruent/incongruent) block, 120 trials of each type during a single run, and 360 trials of each type during the three runs.

MRI Scanning Procedure

Images were acquired using a single shot, spin-echo EPI sequence (TR 2000 ms, TE 75 ms) with 16 axial slices (19.2-cm FOV, 64 by 64 matrix, 5-mm thickness, 1-mm spacing), parallel to the AC-PC plane and covering the whole brain. The geometrical parameters were the same as in the previous study (Zysset *et al.*, 2001). Three functional runs with 365 time points were performed, with each time point sampling over the 16 slices. Prior to the functional runs, the anatomical T_1-weighted MDEFT slices (Norris, 2000) were acquired with the same geometry.

fMRI Data Analysis

The fMRI data were processed using the Lipsia software package (Lohmann *et al.*, 2001), which is based on the general linear model. This contains tools for preprocessing, registration, statistical evaluation, and presentation of fMRI data.

2D motion correction was applied by finding two translational and one rotational parameter that best align each scan of a time sequence, with a reference scan selected by the user. The problem of finding such parameters is formulated as an optimization problem: find parameter values that yield the best match between the current scan and the reference scan. The linear correlation coefficient is used as a matching metric, and Powell's optimization method (Press *et al.*, 1996) is applied to find the best match. Once the parameters have been found, they are applied to the present scan using bilinear interpolation resampling.

To correct for the temporal offset between slices acquired in one scan, a sinc interpolation based on the Nyquist–Shannon Theorem was applied. A temporal highpass filter with a cutoff frequency of 1/180 Hz was used for baseline correction of the signal and a spatial Gaussian filter with $\sigma = 0.8$ was applied. The increased autocorrelation due to filtering was taken into account during statistical evaluation.

To align the functional data slices onto a 3D stereotactic coordinate reference system, a rigid linear registration with 6 degrees of freedom (3 rotational, 3 translational) was performed. The rotational and translational parameters were obtained on the basis of the 2D MDEFT images to achieve an optimal match between these slices and the individual 3D MDEFT reference data set, which had been acquired in a previous session using an established pulse sequence (Lee *et al.*, 1995). The MDEFT volume data set was reconstructed to give 160 slices of 1-mm slice thickness and was standardized to the Talairach stereotactic space. The rotational and translational parameters were normalized, i.e., transformed by linear scaling to a standard size. The resulting parameters were then used to transform the functional slices using trilinear interpolation, so that the resulting functional slices were aligned with the stereotactic coordinate system.

The statistical evaluation was based on a least-squares estimation using the general linear model for serially autocorrelated observations (see also Friston, 1994; Worsley and Friston, 1995; Aguirre *et al.*, 1997; Zarahn *et al.*, 1997). First, for each individual subject, statistical parametric maps were generated and subsequently averaged over all subjects (Bosch, 2000). The design matrix was generated with a boxcar (square wave) function and a response delay of 6 s. The model

equation, including the observation data, the design matrix, and the error term, was convolved with a Gaussian kernel of dispersion of 4 s FWHM. The model includes an estimate of temporal autocorrelation that is used to estimate the effective degrees of freedom (Seber, 1977; Worsley and Friston, 1995). The contrast between the different conditions was calculated using the *t* statistic. Subsequently, *t* values were transformed to *Z* scores. As the individual functional data sets were all aligned to the same stereotactic reference space a group analysis of fMRI data was performed by averaging individual *Z* maps and multiplying each *Z* value with $\sqrt{N}$ (*N* is the number of subjects; Bosch, 2000). Groups of activated pixels were searched for ($Z > 3.1$ and at least four activated pixels) using the method of Braver *et al.* (2001), which also eliminates the requirement to make allowance for multiple comparisons and reduces the sensitivity to false positive activations.

Mechanistic Investigations

Subjects

A total of four healthy volunteers were investigated using the interleaved diffusion-weighted protocol and two using just spin-echo EPI.

MRI Scanning Procedure

In the investigations of the visual cortex a SE-EPI sequence with a 64×64 matrix and a voxel size of $3 \times 3 \times 5$ mm was used (acquisition bandwidth 100 kHz, echo train length 41 ms, TE = 80 ms). Either interleaved diffusion-weighted experiments were performed with a repetition time of 1 s or a simple spin-echo experiment was performed with a repetition time of 2 s. Diffusion weighting was added by inserting a bipolar gradient pair applied simultaneously along the *x*, *y*, and *z* axes with a spacing between the onset of the bipolar gradients of $\Delta = 20$ ms and a duration of $\delta = 15$ ms. The gradient strength was set to give a *b* value of 20 s mm^{-2}. Diffusion weighting was applied in an interleaved fashion, i.e., only on alternate scans. This allows for a better comparison of the BOLD signal and the DW-BOLD signal since the method is less sensitive to the intertrial variability of the subjects (Mildner *et al.*, 2001).

Psychophysical Procedures

For task-induced activation a simple visual task was employed. During periods of control, subjects had to watch a small gray fixation cross positioned in the center of a black screen. To focus attention, subjects had to press a button each time they saw a small black hole appearing in the center of the fixation cross at randomized time intervals. During periods of stimulation, a 7×5 array of red L shapes rotated in a random direction at a frequency of 8 Hz on the black background was presented as a strong visual stimulus while the same attention task had to be performed as during the control periods. The visual stimulus was applied with a duration of 6 s. The recovery period after each stimulus was 54 s. Six complete cycles of visual stimulation were recorded in three slices parallel to and centered in the primary visual cortex. One complete dummy cycle, i.e., stimulation, RF pulses, and gradient noise, was performed before data recording was commenced.

fMRI Data Analysis

The processing of the data was performed as follows: The image time series was first corrected for bulk motion using a motion correction routine incorporated in the Lipsia software package (Lohmann *et al.*, 2001). A high-pass filter was applied in order to remove possible drifts of the baseline. The data set was then divided into two sets, one with and another without diffusion weighting. The two data sets obtained have a time resolution of 2 s and the diffusion-weighted data set is delayed by 1 s. The activated brain regions for both data sets were selected by correlating the time course of each voxel of the non-diffusion-weighted data set with a design function representing the characteristics of the stimulus. The time points of the design function from 6 to 12 s after stimulation were referred to as the activated state and the last 20 s of the resting period were referred to as the resting state. For the correlation analysis, the time points during the transition period between the activated and the resting states were ignored. Voxels having a correlation coefficient above 0.4 were chosen as the activated voxels for all subjects. After averaging the six cycles of visual stimulation and rest, the time courses for all activated voxels were averaged in order to give the BOLD signal and the DW-BOLD signal.

RESULTS

In the Stroop experiment all regions of activation that had previously been detected using GE-EPI (Zysset *et al.*, 2001) were present in the SE-EPI data. A detailed description of the areas of activation is to be found in Table 1, which also gives the means and variances of the *Z* scores. Data are shown for the incongruent versus the neutral condition. Comparison between the other conditions did not yield any different areas of activation. For illustrative purposes Fig. 2 shows SE-EPI and GE-EPI images from the region in question. Additional activation was detected with SE-EPI in the ventral frontomedian cortex as shown in Fig. 3 and in the right frontopolar cortex (cf. Table 1). A small region of artifactual activation is visible outside the brain in Fig. 3, which is probably caused by coherent eye movement: the eyes may clearly be im-

TABLE 1

Talairach Coordinates, Maximum *Z* Value of the Local Maxima and Volume of the Activated Regions for Neutral vs Incongruent

	GE-EPI				SE-EPI			
Area	*x*	*y*	*z*	*Z* max	*x*	*y*	*z*	*Z* max
pre-SMA	1	26	42	8.90	−1	25	43	4.65
L post. inferior frontal sulcus	−38	5	30	12.55	−38	4	33	5.58
R post. middle frontal gyrus	44	15	36	9.00	39	17	21	3.66*
L ant. inferior frontal sulcus	−38	35	5	7.79	−43	41	4	5.20
R frontopolar cortex	31	53	15	8.67	19	62	11	3.39*
L intraparietal sulcus	−21	−77	43	11.52	−26	−63	44	6.72
R intraparietal sulcus	25	−69	44	10.78	25	−71	37	5.63
L lateral occipitotemporal gyrus	−38	−72	1	9.77	−44	−77	3	5.25
R lateral occipitotemporal gyrus	40	−73	−2	9.92	38	−81	4	4.75
R frontopolar cortex					−11	67	13	5.20
Ventral frontomedian cortex					−4	50	2	−5.50
Mean				9.88				5.05
Variance				2.28				0.86

Note. *Z* values were thresholded at $Z > 6.5$ for GE-EPI and at $Z > 3.1$ for SE-EPI. Clusters had a minimum size of 180 pixels. Regions denoted by (*) were smaller then 180 pixels. The mean and variance of the *Z* values taken over all the areas are also given.

aged in SE-EPI, but are generally not seen in GE-EPI. The ventral frontomedian activation is shown as blue in Fig. 3 because the activation was stronger in the neutral than in the incongruent condition. The level of activation in this area is known to decrease during cognitive tasks with a high attentional load, as this area is believed to be associated with a default mode of brain activity (Raichle *et al.*, 2001). The frontopolar activation is related to volitional, strenuous processing and problem solving (Goel *et al.*, 1997). Activation in these regions is not normally detectable on standard GE-EPI data because of the presence of strong susceptibility gradients. The *Z*-score values were, however, significantly reduced from those values recorded in the GE-EPI experiment: for equivalent experimental conditions it is to be expected that the *Z* scores will fall by a factor of about 3. The numerical values presented in Table 1 are about a factor of 2 lower, but in the previous study (Zysset *et al.*, 2001) nine subjects were investigated, with each investigation consisting of two runs each containing four blocks, whereas here seven subjects were examined with three repetitions and six blocks. The activation in the SE-EPI images appears more focused than in GE-EPI, and the variance of the *Z* scores as shown in Table 1 is lower. One example of the difference in the quality of activation is shown in Fig. 4, which shows the activation in the left anterior and posterior inferior frontal sulcus (IFS). In the GE-EPI data the anterior activation is lower both in extent and in maximum *Z* score compared to the posterior activation. In the SE-EPI images the activation is more similar. A probable explanation for this is that the anterior IFS is in a region where the main magnetic field homogeneity is likely to be degraded by susceptibility gradients.

Representative time courses from the experiments in the visual cortex are shown in Fig. 5. The top diagram shows that the mild diffusion weighting used results in an approximately 50% reduction in the relative signal change arising from visual stimulation. The bottom plot shows that a clear poststimulus undershoot can be detected.

DISCUSSION

In this paper it has been shown for the first time that SE-EPI at 3 T is sufficiently sensitive to be used in a cognitive fMRI study, albeit with a reduction in *Z* score of about a factor of 3, when the different powers of the two experiments are taken into account. Despite this, it was possible to perform a study using just seven volunteers that yielded results similar to those of the previously published GE-EPI study (Zysset *et al.*, 2001). Comparing the results presented in this paper with those of the previous study it should be borne in mind that this is a historical comparison, as indicated in the Introduction; the aim of this paper is to assess the utility of SE-EPI at 3 T for cognitive studies. The use of different subjects automatically means that the extent and degree of activation will not be identical. If it were desired to perform a direct comparison then either GE-EPI and SE-EPI would have to be performed sequentially on the same subjects within a session or a pulse sequence for simultaneous acquisition of GE-EPI and SE-EPI would have to be implemented (Bandettini *et al.*, 1993).

The auxiliary experiments performed in the visual cortex demonstrated that extravascular signal changes contribute about half of the total signal change. The qualitative appearance of the data is that they are

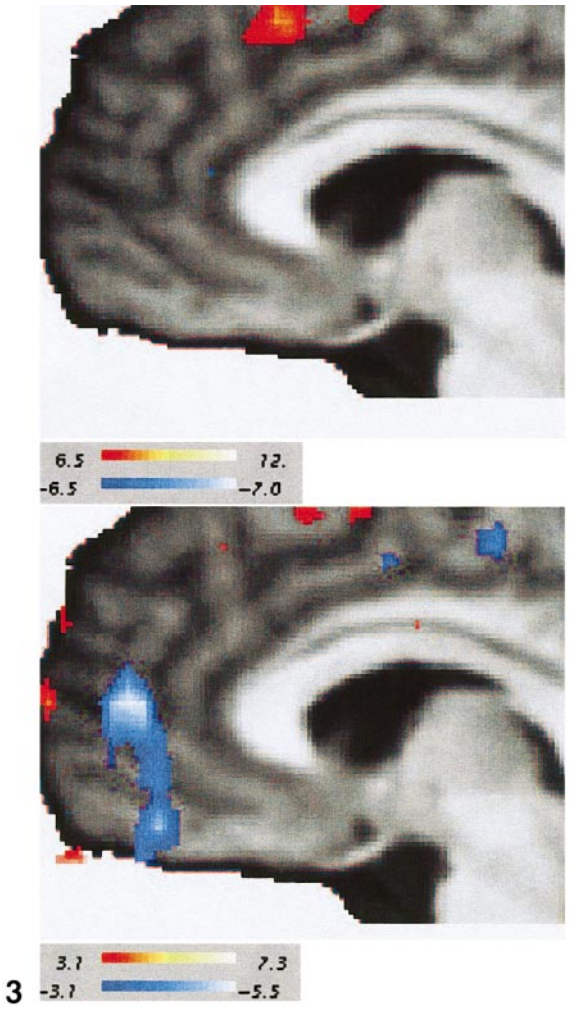

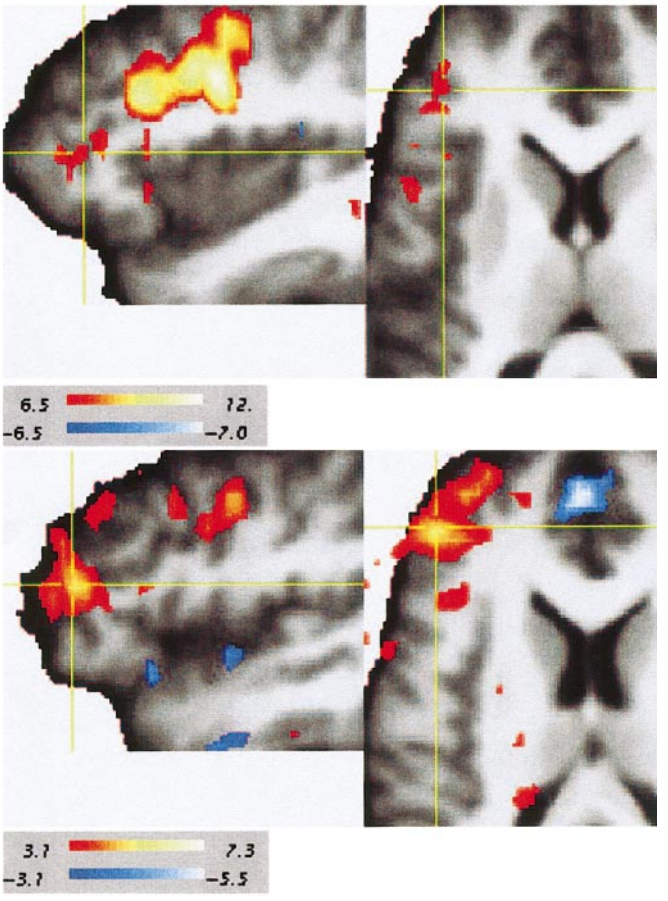

FIG. 3. Sagittal activation maps. The top image was obtained with GE-EPI, the bottom image with SE-EPI. The slice is positioned at Talairach coordinate $z = -5$. The ventral frontomedian activation is clearly visible in the SE-EPI image, but not in the GE-EPI image due to the strong susceptibility gradients in this region which result in signal voids in the GE-EPI data, particularly in the most inferior slices. Activation in the pre-SMA region is visible with both imaging sequences.

FIG. 4. Sagittal and axial slices obtained with GE-EPI (top) and SE-EPI (bottom). The yellow axes intersect at the Talairach coordinates (−38, 35, 5) for the GE-EPI image and (−43, 41, 4) for the SE-EPI image. These are the coordinates of the left anterior inferior frontal sulcus (IFS), as can be seen by reference to Table 1. The other activated region shown corresponds to the left posterior IFS. In GE-EPI the activation in the posterior IFS is dominant, whereas in SE-EPI the levels of activation at the two locations are similar.

better localized to the cortex, a result that is in accordance with those previously obtained by Thulborn *et al.* (1997) in the visual cortex at 3 T. This does not exclude the possibility that some voxels which contain larger blood vessels will give significant signal changes in signal intensity in SE-EPI as a result of the changes in T_2, as found by Prinster *et al.* (1997) and Oja *et al.* (1999). If necessary the signal from these vessels could be removed by the application of a mild diffusion weighting (Boxerman *et al.*, 1995) at the cost of a further reduction in sensitivity. Functional MRI at 3 T using SE-EPI is hence in an intermediate regime compared to 1.5 T, at which diffusion weighting will eliminate almost the entire signal change (Jones, 1999), and very high field strengths such as 9.4 T (Lee *et al.*, 1999), at which the BOLD signal is almost exclusively extravascular in origin. A mild diffusion weighting such as applied here will be sufficient only to remove the signal from postcapillary vessels; the possibility still remains that the remaining signal change could arise from within the capillaries, and such an explanation has been postulated for the signal undershoot at 1.5 T (Jones, 1999).

The use of SE-EPI requires a TE which is roughly equal to the T_2 of the tissue being examined (Bandettini *et al.*, 1994), whereas for GE-EPI the optimum TE is T_2^*. This reduces the number of slices per unit time that can be acquired: for our system and the imaging parameters used in this study the reduction is from 14 to 10 slices per second. The images acquired will still

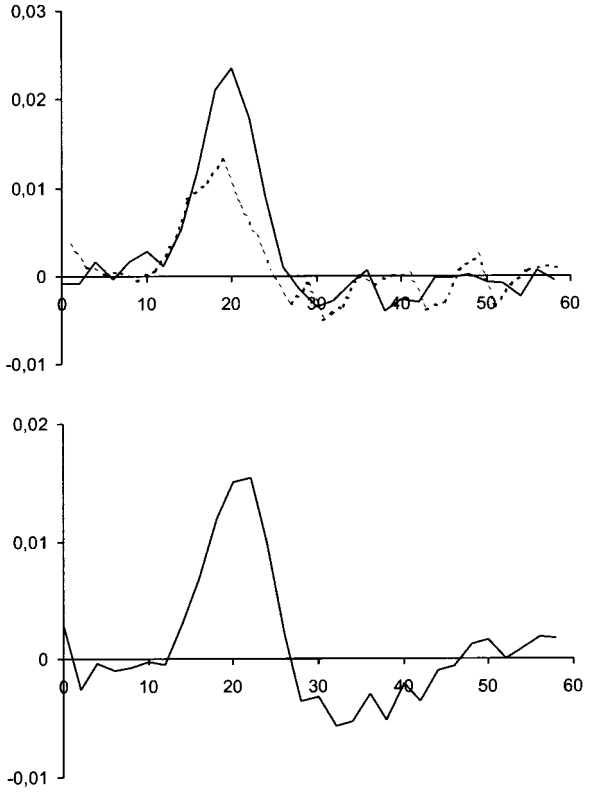

FIG. 5. Time courses of the BOLD response in the visual cortex. The top shows the result of an interleaved measurement with and without diffusion weighting at a b value of 20 s mm^{-2}. The diffusion-weighted time course is shown in dotted lines. Signal arising from blood vessels will largely be eliminated by the diffusion weighting; the residual signal arises from the extravascular space. The bottom shows a single time course, the poststimulus undershoot is clearly visible here.

suffer from the same distortions as GE-EPI, but without the signal voids. In this study the disappearance of the signal voids was sufficient to detect two regions of frontal activation that were previously not visible in a GE-EPI study (Zysset *et al.*, 2001). The Stroop paradigm employed here was chosen because of its robustness and not because it was primarily expected to generate ventromedial activation. That such activation was found is in itself not surprising as this region is generally believed to be associated with anticipatory activity, problem solving, and decision-making (Bechara *et al.*, 1997, 1998; Goel *et al.*, 1997; Raichle *et al.*, 2001). The use of a fast spin-echo or RARE sequence as advocated by Constable *et al.* (1994) with a short inter-echo TE and a long preparation TE would eliminate all distortion but further reduce the number of slices per second. One potential advantage of using T_2 contrast is, as mentioned in the Introduction, that the value of T_2 varies little between gray matter regions in the brain. The sensitivity of the experiment should hence be independent of position, in marked contrast to GE-EPI, in which a large variation in T_2^* values is to be expected. This presumably accounts for the greater variance in the Z scores between regions for GE-EPI than for SE-EPI, as is shown in Table 1, and the difference between the relative degrees of activation between the posterior and the anterior left IFS as documented in Fig. 4. It is of course clear that the variation in T_2^* values is primarily due to extrinsic factors and that if these can be compensated then the intrinsic variation will be less (Deichmann and Turner, 2001); however, schemes for assessing the intrinsic variation will generally lengthen the experimental procedure.

In conclusion, the use of T_2-weighted fMR at 3 T is to be advocated where activation is to be expected in regions which suffer from susceptibility gradients and where a high degree of spatial localization is necessary. It will not be the method of choice where maximum sensitivity is required, particularly in regions of the brain with good main field homogeneity. Although the sensitivity of T_2-weighted fMR at 1.5 T is probably too low for use in cognitive studies, at field strengths of 3 T and above it should prove a valuable alternative to the more conventional T_2^*-weighted sequences and make the ventromedial cortex more readily accessible to fMRI investigations.

ACKNOWLEDGMENT

The authors thank Professor D. Y. von Cramon for helpful discussions regarding the content of the manuscript.

REFERENCES

Aguirre, G. K., Zarahn, E., and d'Esposito, M. 1997. Empirical analyses of BOLD fMRI statistics. II. Spatially smoothed data collected under null-hypothesis and experimental conditions. *NeuroImage* **5:** 199–212.

Bandettini, P. A., Wong, E. C., Jesmanowicz, A., Hinks, R. S., and Hyde, J. S. 1993. Simultaneous mapping of activation induced ΔR2* and ΔR2 in the human brain using a combined gradient-echo and spin-echo EPI pulse sequence. In *Proceedings: 12th Meeting of the Society of Magnetic Resonance in Medicine*, New York, p. 169.

Bandettini, P. A., Wong, E. C., Jesmanowicz, A., Hinks, R. S., and Hyde, J. S. 1994. Spin-echo and gradient-echo EPI of human brain activation using BOLD contrast: A comparative study at 1.5 T. *NMR Biomed.* **7:** 12–20.

Bechara, A., Damasio, H., Tranel, D., and Anderson, S. W. 1998. Dissociation of working memory from decision making within the human prefrontal cortex. *J. Neurosci.* **18:** 428–437.

Bechara, A., Damasio, H., Tranel, D., and Damasio, A. R. 1997. Deciding advantageously before knowing the advantageous strategy. *Science* **275:** 1293–1295.

Bosch, V. 2000. Statistical analysis of multi-subject fMRI data: The assessment of focal activations. *J. Magn. Reson. Imaging* **11:** 61–64.

Boxerman, J. L., Bandettini, P. A., Kwong, K. K., Baker, J. R., Davis, T. L., Rosen, B. R., and Weisskoff, R. M. 1995. The intravascular contribution to fMRI signal change: Monte Carlo modeling and diffusion-weighted studies in vivo. *Magn. Reson. Med.* **34:** 4–10.

Braver, T. S., Barch, D. M., Kelley, W. M., Buckner, R. L., Cohen, N. J., Miezin, F. M., Snyder, A. Z., Ollinger, J. M., Akbudak, E., Conturo, T. E., and Petersen, S. E. 2001. Direct comparison of prefrontal cortex regions engaged by working and long-term memory tasks. *NeuroImage* **14:** 48–59.

Buxton, R. B., Wong, E. C., and Frank, L. R. 1998. Dynamics of blood flow and oxygenation changes during brain activation: The balloon model. *Magn. Reson. Med.* **39:** 855–864.

Constable, R. T., Kennan, R. P., Puce, A., McCarthy, G., and Gore, J. C. 1994. Functional NMR imaging using fast spin echo at 1.5 T. *Magn. Reson. Med.* **31:** 686–690.

Deichmann, R., and Turner, R. 2001. Compensation of susceptibility induced bold sensitivity losses in echo-planar fMRI imaging. In *Proceedings: 9th Meeting of the International Society for Magnetic Resonance in Medicine,* Glasgow, p. 1234.

Friston, K. J. 1994. Statistical parametric maps in functional imaging: A general linear approach. *Hum. Brain. Mapp.* **2:** 189–210.

Goel, V., Gold, B., Kapur, S., and Houle, S. 1997. The seats of reason? An imaging study of deductive and inductive reasoning. *NeuroReport* **8:** 1305–1310.

Hennig, J., Nauerth, A., and Friedburg, H. 1986. RARE imaging: A fast imaging method for clinical MR. *Magn. Reson. Med.* **3:** 823–833.

Jones, R. A. 1999. Origin of the signal undershoot in BOLD studies of the visual cortex. *NMR Biomed.* **12:** 299–308.

Jones, R. A., Schirmer, T., Lipinski, B., Elbel, G. K., and Auer, D. P. 1998. Signal undershoots following visual stimulation: A comparison of gradient and spin-echo BOLD sequences. *Magn. Reson. Med.* **40:** 112–118.

Kavec, M., Gröhn, O. H. J., Kettunen, M. I., Silvennoinen, M. J., Penttonen, M., and Kauppinen, R. A. 2001. Use of spin echo T_2 BOLD in assessment of cerebral misery perfusion at 1.5 T. *Magma* **12:** 32–39.

Lee, J.-H., Garwood, M., Menon, R., Adriany, G., Andersen, P., Truwit, C. L., and Uğurbil, K. 1995. High contrast and fast three-dimensional magnetic resonance imaging at high fields. *Magn. Reson. Med.* **34:** 308–312.

Lee, S. P., Silva, A. C., Uğurbil, K., and Kim, S. G. 1999. Diffusion-weighted spin-echo fMRI at 9.4 T: Microvascular/tissue contribution to BOLD signal changes. *Magn. Reson. Med.* **42:** 919–928.

Lohmann, G., Mueller, K., Bosch, V., Mentzel, H., Hessler, S., Chen, L., Zysset, S., and von Cramon, D. Y. 2001. Lipsia—A new software system for the evaluation of functional magnetic resonance images of the human brain. *Comput. Med. Imaging Graph.* **25**.

Lowe, M. J., Lurito, J. T., Mathews, V. P., Phillips, M. D., and Hutchins, G. D. 2000. Quantitative comparison of functional contrast from BOLD-weighted spin-echo and gradient-echo echo-planar imaging at 1.5 Tesla and $H_2{}^{15}O$ PET in the whole brain. *J. Cereb. Blood Flow Metab.* **20:** 1331–1340.

Mildner, T., Norris, D. G., Schwarzbauer, C., and Wiggins, C. J. 2001. A qualitative test of the balloon model for BOLD-based MR signal changes at 3 Tesla. *Magn. Reson. Med.* **46:** 891–899.

Norris, D. G. 2000. Reduced power multislice MDEFT imaging. *J. Magn. Reson. Imaging* **11:** 445–451.

Oja, J. M., Gillen, J., Kauppinen, R. A., Kraut, M., and van Zijl, P. C. M. 1999. Venous blood effects in spin-echo fMRI of human brain. *Magn. Reson. Med.* **42:** 617–626.

Press, W., Teukolsky, S., Vetterling, W., and Flannery, B. 1996. *Numerical Recipes in C,* 2nd ed. Cambridge Univ. Press, Cambridge, UK.

Prinster, A., Pierpaoli, C., Turner, R., and Jezzard, P. 1997. Simultaneous measurement of $\Delta R2$ and $\Delta R2^*$ in cat brain during hypoxia and hypercapnia. *NeuroImage* **6:** 191–200.

Raichle, M. E., MacLeod, A. M., Snyder, A. Z., Powers, W. J., Gusnard, D. A., and Shulman, G. L. 2001. A default mode of brain function. *Proc. Natl. Acad. Sci. USA* **98:** 676–682.

Seber, G. A. F. 1977. *Linear Regression Analysis*. Wiley, New York.

Thulborn, K. R., Chang, S. Y., Shen, G. X., and Voyvodic, J. T. 1997. High-resolution echo-planar fMRI of human visual cortex at 3.0 tesla. *NMR Biomed.* **10:** 183–190.

Treisman, A. M., and Fearnley, S. 1969. The Stroop test: Selective attention to colours and words. *Nature* **222:** 437–439.

Worsley, K., and Friston, K. 1995. Analysis of fMRI time-series revisited—Again. *NeuroImage* **2:** 359–365.

Wright, G. A., Hu, B. S., and Macovski, A. 1991. Estimating oxygen saturation of blood in vivo with MR imaging at 1.5 T. *J. Magn. Reson. Imaging* **1:** 275–283.

Zarahn, E., Aguirre, G. K., and d'Esposito, M. 1997. Empirical analyses of BOLD fMRI statistics. I. Spatially unsmoothed data collected under null-hypothesis conditions. *NeuroImage* **5:** 179–197.

van Zijl, P. C. M., Eleff, S. M., Ulatowski, J. A., Oja, J. M., Ulug, A. M., and Kauppinen, R. A. 1998. Quantitative assessment of blood flow, blood volume and blood oxygenation effects in functional magnetic resonance imaging. *Nat. Med.* **4:** 159–167.

Zysset, S., Müller, K., Lohmann, G., and von Cramon, D. Y. 2001. Color-word matching Stroop task: Separating interference and response conflict. *NeuroImage* **13:** 29–36.